

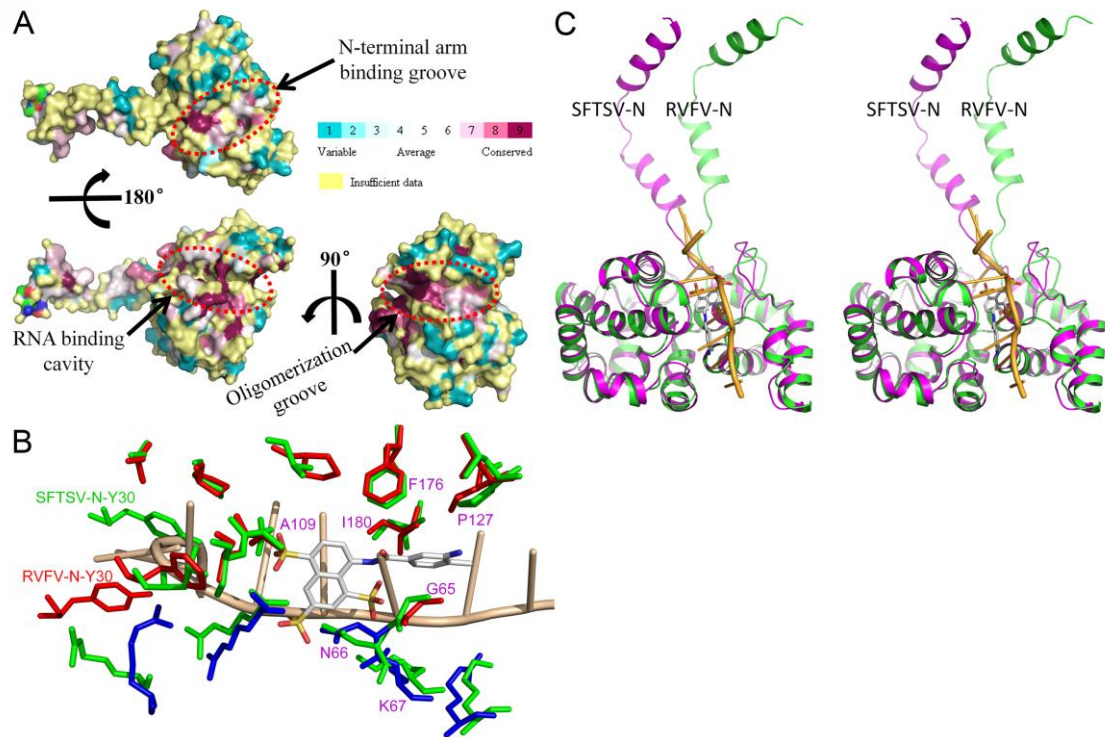
**B**

Mutations		$A_{260}/A_{280}$	Oligomerization state
SFTSV-N	Native WT	1.23	Hexamer/Pentamer
	Partial unfolding	0.6	Hexamer/Pentamer
	K67Q	0.52	Hexamer/Pentamer
	K67D	0.49	Hexamer/Pentamer
	R64D/K67D/K74D	0.48	Tetramer
GRAV-N	WT	1.33	Hexamer/Pentamer
	Partial unfolding	0.62	Hexamer/Pentamer
	R69D/K72E/K79E	0.55	Tetramer
BUEV-N	WT	1.31	Hexamer/Tetramer
	Partial unfolding	0.66	Hexamer/Tetramer
	R63D/K66E/K73E	0.56	Hexamer

1

2 **Figure S1** Native and mutant Ns bind with various amount of RNA from *E. coli*. (A)  
 3 Size exclusion chromatography (SEC) of SFTSV-N, GRAV-N and BUEV-N. Samples  
 4 of SFTSV-N, triple mutant SFTSV-N (3mSFTSV-N), GRAV-N and BUEV-N in  
 5 complex with *E.coli* RNA, SFTSV-N in complex with Suramin and RNA-free  
 6 SFTSV-N were injected, respectively, onto a Superdex G200 (120 ml) column. (B)  
 7  $A_{260}/A_{280}$  ratios and corresponding oligomerization states of native and mutant Ns bind  
 8 with RNA from *E. coli*.

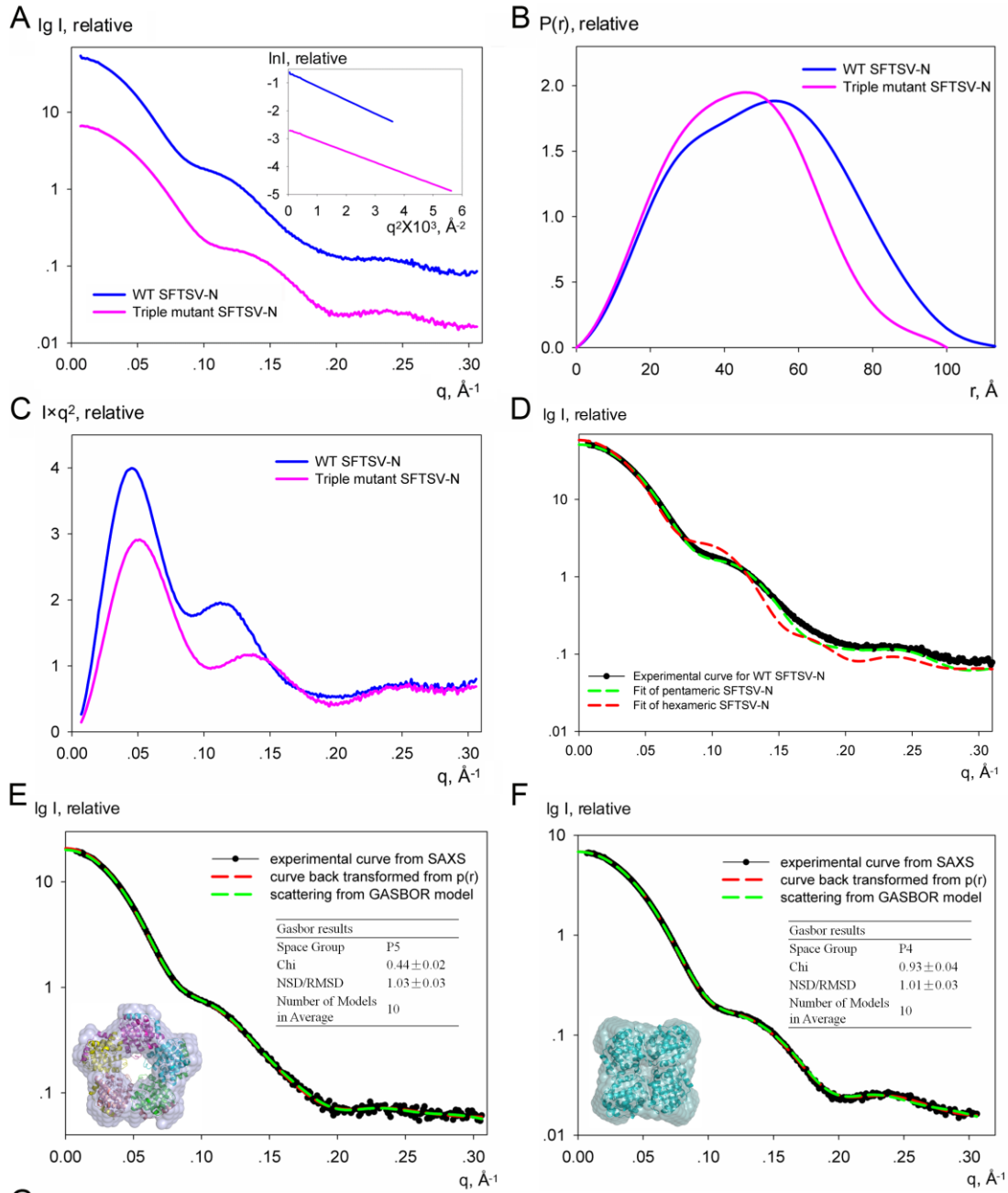
9



10

11 **Figure S2** Conserved structures of phleboviral Ns and comparison between  
 12 RVFV-N:RNA and SFTSV-N:Suramin complexes. (A) Residues on the surface of  
 13 RNA binding cavity, oligomerization groove, interfaces between N-terminal arm and  
 14 its binding groove are highly conserved. Amino acid conservation of phleboviral Ns is  
 15 displayed on the WT SFTSV-N structure by ConSurf (<http://consurf.tau.ac.il/>). (B)  
 16 Residues in the RNA binding cavity of RVFV-N (PDB code: 4H5O, residues  
 17 contributing to hydrophobic interactions are shown in red, while those involved in  
 18 formation of polar contacts are shown in blue) and their comparison with  
 19 corresponding residues on SFTSV-N (green). Suramin and RNA are showed in white  
 20 and light orange, separately. The magenta labels indicate the six RNA binding  
 21 residues in RVFV-N which are identical with the corresponding conserved residues  
 22 found in SFTSV-N for binding Suramin. Side chain orientation of Y30 is dependent  
 23 on the N-terminal arm flexibility. (C) Stereo view of superimposed structures of  
 24 RVFV-N: RNA complex (PDB code: 4H5O) in magenta and light orange onto  
 25 SFTSV-N: Suramin complex in green and white.

26

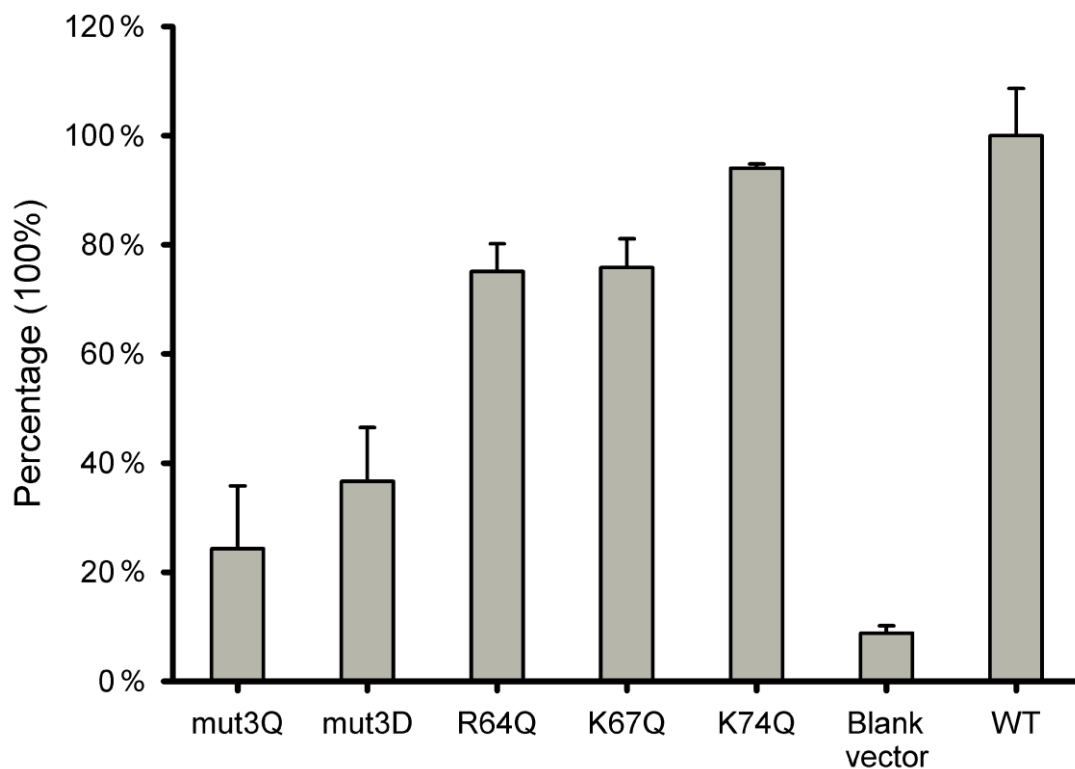


27

28 **Figure S3** SAXS analysis of WT SFTSV-N and triple mutant SFTSV-N. (A)  
 29 Scattering curves of SFTSV-N generated by averaging nine experimental datasets,  
 30 including: WT SFTSV-N (blue) and triple mutant SFTSV-N (magenta). The inset  
 31 figure is Guinier plots. The wide  $q$  range linearity in the plots,  $\ln[I(q)]$  vs  $q^2$ , suggests  
 32 that there was neither detectable inter-particle interactions nor radiation damage

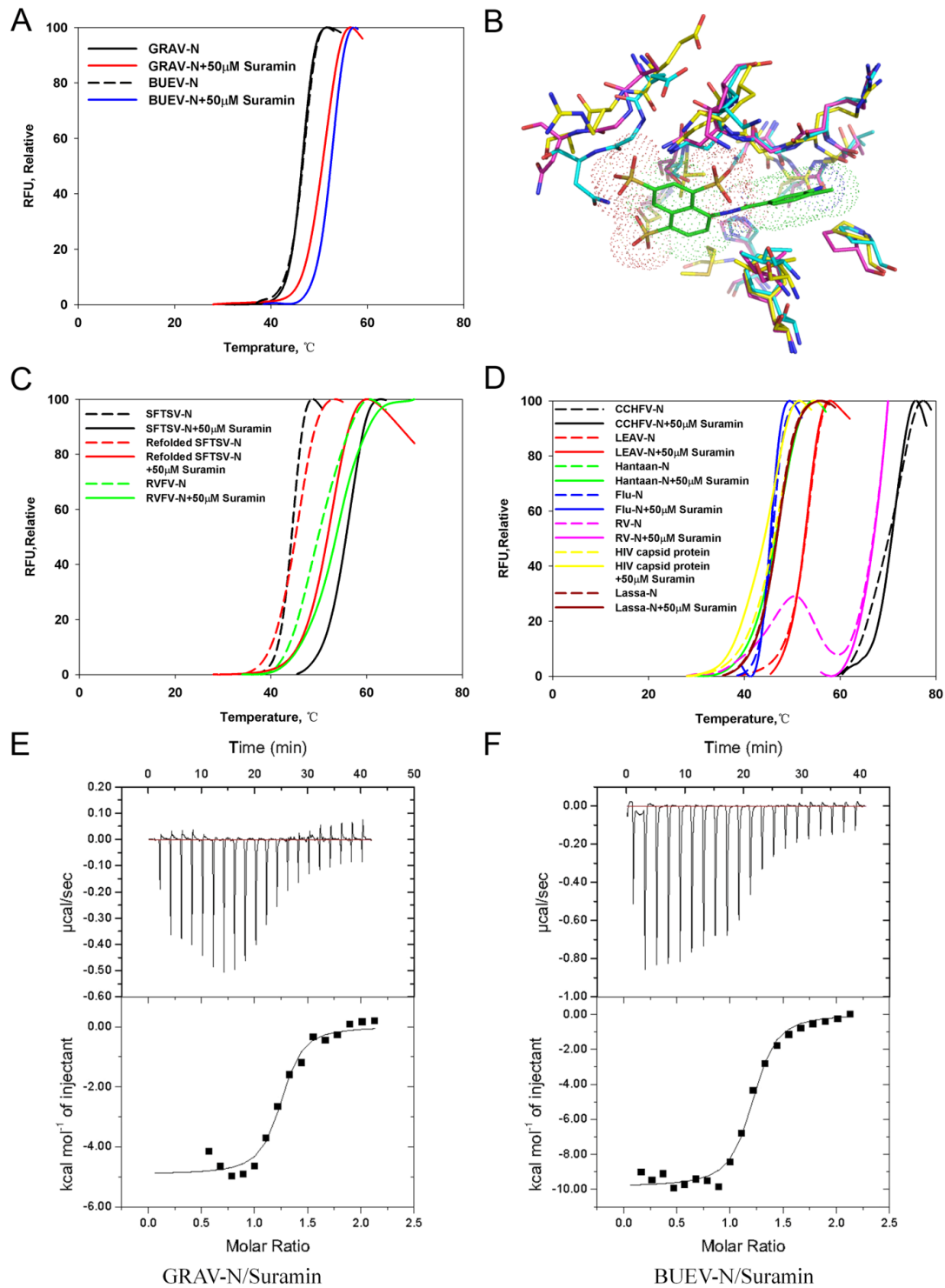
33 during collection of SAXS data. (B) Pair distance distribution function,  $P(r)$ , curves.  
 34 (C) Kratky plots. The bell-shaped kratky curves demonstrate the proteins were well  
 35 folded. (D) Fits generated by CRY SOL between experimental scattering curve and  
 36 pentamer or hexamer observed in crystal packing. GASBOR models for WT  
 37 SFTSV-N (E) and triple mutant SFTSV-N (F) were obtained from averaging 10  
 38 models calculated by GASBOR individually. The crystal structures of pentameric WT  
 39 SFTSV-N and tetrameric triple mutant SFTSV-N were superimposed into the  
 40 GASBOR models by SUPCOMB. (E) Pentameric model for WT SFTSV-N with P5  
 41 symmetry as a restraint. (F) SAXS model for triple mutant SFTSV-N using P4  
 42 symmetry. The goodness-of-fitness parameter Chi and the NSD/RMSD of 10 models  
 43 are listed in the table (inset). (G) Parameters derived from SAXS curves.  $R_g$  and  $D_{max}$   
 44 are estimated by calculating  $P(r)$  using GNOM.  $V_{Porod}$  is calculated using PRIMUS.  
 45 The calculated shape  $R_g$  was generated by CRY SOL. The molecular weights (MWs)  
 46 were predicted using the web server (<http://www.if.sc.usp.br/~saxs/saxsmow.html>).  
 47 All the values with error bars are from three replicate samples.

48



49

50 **Figure S4** Ability of WT SFTSV-N and a panel of N mutants to transcribe the M  
 51 reporter gene were evaluated by the luciferase assay in 293T cells. mut3Q:  
 52 R64Q/K67Q/K74Q; mut3Q: R64D/K67D/K74D.



53

54 **Figure S5** Suramin specifically binds pleboviral Ns. (A) GRAV-N and BUEV-N  
 55 bind Suramin as measured by thermal shift assays. (B) The residues within 5 Å  
 56 of Suramin derived from WT SFTSV-N: Suramin complex and the corresponding  
 57 residues from GRAV-N and BUEV-N. Specificity of Suramin for (C) Bunyavirus Ns  
 58 and (D) N from other viruses as measured by thermal shift assays. LEAV-N: Leayer  
 59 virus N (*Orthobunyavirus* genus); Hantaan-N: Hantaan virus N (*Hantavirus* genus);

60 flu-N: Influenza A virus N; RV-N: Rabies virus N; Lassa-N: Lassa virus N. (E)

61 GRAV-N and (F) BUEV-N bind with Suramin as confirmed by ITC.

62

63

64

65 TABLE S1 SFTSV N-N protomer interface hydrogen bonds (distances  $\leq 3.2$  Å)

66

<b>N-N protomer</b>	<b>Chain A residue/atom</b>	<b>Chain B residue/atom</b>	<b>Hydrogen bond Distance (Å)</b>
<b>WT SFTSV-N (P6)</b>	SER5/OG	PHE209/O	2.53
	GLN14/OE1	LYS55/NZ	2.77
	GLU20/OE2	LYS52/NZ	2.28
	ARG26/NH1	TYR125/OH	3.07
	GLU27/O	SER76/OG	2.74
	LEU29/O	ARG64/NH1	2.69
	GLU31/N	LYS74/O	2.96
	ARG99/NH1	MET75/O	2.45
	ARG99/NH2	MET75/O	2.77
	ARG99/NH2	SER72/O	3.00
<b>Triple mutant SFTSV N</b>	ASP64/OD2	LEU28/O	2.76
	ASP74/O	ARG99/NH2	2.79
	ASP74/OD1	GLY32/O	3.00
	SER76/OG	GLU27/O	2.55
	LYS184/O	ASN182/ND2	2.71
	PHE209/O	SER5/OG	2.80

67

68

69 TABLE S2 Residues in the RNA binding cavity of RVFV-N and their comparison  
 70 with corresponding residues on SFTSV-N, GRAV-N and BUEV-N.

71

SFTSV-N	GRAV-N	BUEV-N	RVFV-N
Y30	Y32	Y29	Y30
L33	F35	F32	F33
G65	G70	G64	G65
Q109	A114	A108	A109
S110	A115	A109	A110
L126	L131	L125	L126
P127	P132	P126	P127
A148	P153	P146	P147
F177	F182	F175	F176
I181	I186	I179	I180
P200	P205	P198	P199
A203	A208	A201	A202
N66	N71	N65	N66
K67	K72	K66	K67
K70	K75	K69	R70
R99	R104	R98	R99
R106	R111	R105	R106

72 The six residues in red color are responsible to bind both Suramin and RNA  
 73 potentially.

74  **Strictly conserved residues.**

75  **Conserved residues.**

76

77

78



79 TABLE S3 Residues of SFTSV-N contact with Suramin within 5.0 Å and their  
 80 comparison with corresponding residues on GRAV-N, BUEV-N and RVFV-N.

81

SFTSV-N	GRAV-N	BUEV-N	RVFV-N
A61	N66	S60	A61
L62	L67	L61	L62
T63	V68	T62	T63
R64	R69	R63	R64
G65	G70	G64	G65
N66	N71	N65	N66
K67	K72	K66	K67
E94	E99	S93	E94
R95	G100	G94	G95
A96	N101	N95	N96
V105	S110	S104	S105
Q109	A114	A108	A109
P127	P132	P126	P127
M147	H152	H145	H146
F177	F182	F175	F176
I181	I186	I179	I180

82 The six residues in red color are responsible to bind both Suramin and RNA  
 83 potentially.

84

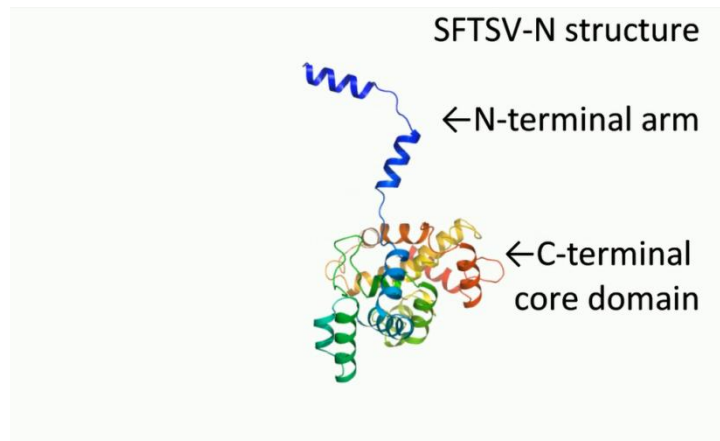
 **Strictly conserved residues.**

85

 **Conserved residues.**

86

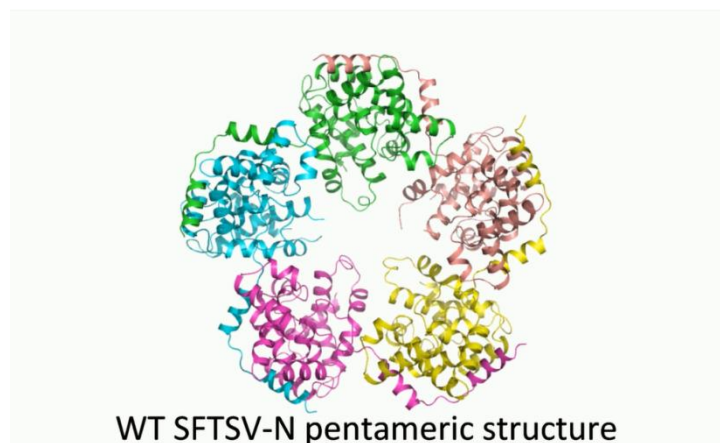
87 **Movie legends**



88

89 **Movie S1:** SFTSV-N wild type and triple mutant monomer structures. Three  
90 mutated residues are shown as sticks.

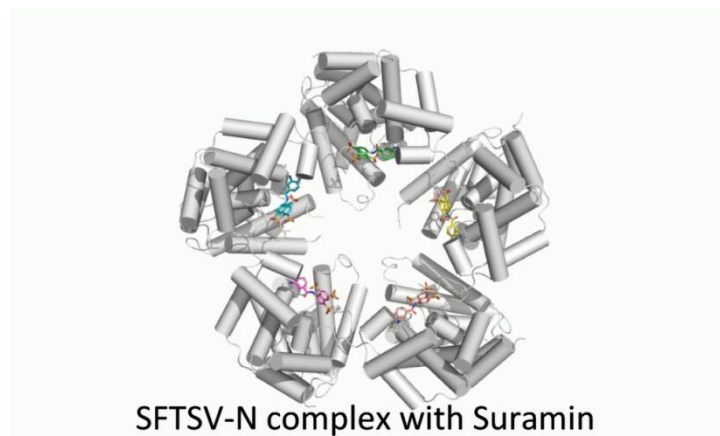
91



92

93 **Movie S2:** The wild type SFTSV-N pentamer structure is shown as ribbon and  
94 electrostatic potential surface representation.

95



96

97 **Movie S3:** SFTSV-N complex with Suramin and detailed interactions are shown.